NASA TECHNICAL MEMORANDUM

NASA TM-73807

NASA TM-73807

DISTRIBUTION OF E/N AND N_e IN A CROSS-FLOW ELECTRIC DISCHARGE LASER

by John W. Dunning, Jr., Richard B. Lancashire, and Eugene J. Manista
Lewis Research Center
Cleveland, Ohio 44135

TECHNICAL PAPER presented at the
Twenty-ninth Annual Gaseous Electronics Conference
sponsored by the General Electric Company and the American Physical Society
Cleveland, Ohio, October 19-22, 1976.

DISTRIBUTION OF E/N and N_e IN A CROSS-FLOW ELECTRIC DISCHARGE LASER

by John W. Dunning, Jr., Richard B. Lancashire, and Eugene J. Manista

ABSTRACT

The spatial distribution of the ratio of electric field to neutral gas density in a flowing gas, multiple pin-to-plane discharge was measured in the high-power, closed-loop laser at the NASA Lewis Research Center. The laser was operated at a pressure of 140 torr (1:7:20, CO_2, N_2, He) with typically a 100 meter/second velocity in the 5 x 8 x 135 centimeter discharge volume. E/N ratios ranged from 2.7×10^{-16} to 1.4×10^{-16} volts-cm^2 along the discharge while the electron density ranged from 2.8×10^{10} to 1.2×10^{10} cm^{-3}.

INTRODUCTION

E-9390

The National Aeronautics and Space Administration (NASA) is engaged in a high-power laser research program whose purpose is to define and evaluate the potential of high power lasers for NASA applications. In support of this program, research and development activities are being conducted in several key areas; one such area is that of CO_2 laser technology. As part of this effort, NASA-Lewis designed and fabricated a CO_2, electric-discharge, closed-cycle laser system.

The discharge properties must be varied in the direction of the flow to provide optimum laser performance (e.g., discharge stability and matching of the discharge E/N to the laser kinetics) (Weigand, Ref. 1). One of the phenomena which makes it difficult to predict the discharge properties and thus the laser performance is the convection of ions and electrons downstream of an individual discharge. Effects of this convection in a small scale discharge have been reported (Wutzke and Pack, Ref. 2). The first measurements of the effect of this convection on the discharge in a large scale laser are presented in this report. The results are presented for one particular distribution of ballast resistance. This distribution was chosen because it provided a reasonably good beam profile at a total discharge current of 11 amperes and a velocity of 90 m/sec.

Measurements were made of discharge properties from

which values of electric field, current density, input power density, ratio of electric field to neutral gas density (E/N), and electron number density (N_e) were calculated.

THE LEWIS HIGH POWER LASER

A complete description of the laser flow loop, its supporting equipment, and its capabilities is given in Reference 3. A sketch of the facility is shown in Figure 1 to show the position of the laser test cavity relative to the other components of the flow loop. This test cavity is configured for multiple pin-to-plate discharge excitation of the flowing CO_2 laser gas mixture and is shown in Figure 2. The directions of the discharge, optics, and flow are mutually orthogonal. The laser test cavity consists of five major components; the main frame, the bellmouth entrance, the cathode, the anode, and the optics. The mainframe is a structure which connects the electrode sections, mirror mounts, and flow loop. It is approximately 1.4 meters in the flow direction by 1.5 meters in the optics direction. For the data presented here, the spacing between the cathode and the anode frames was 6 centimeters. The mainframe is electrically isolated from the rest of the flow loop. The internal sidewalls are lined with NEMA G-10 to minimize arc attachment to bare metal. The bell mouth is inserted into the upstream opening of the mainframe to aerodynamically tailor the gas stream entering the cavity.

The cathode section consists of a stainless steel frame whose dimensions are 1 x 1.5 meters. Although the frame allows for five separate pin-to-plate discharge sections, only the middle section was operating in the present series of tests. The surface of the frame which is exposed to the discharge is coated with an epoxy material. The pins are epoxied into the panels in rows and columns forming an hexagonal array with a pin density of one pin per square centimeter. The pins, which were made from 1.5 millimeter diameter tungsten-3% rhenium wire, are pointed and protrude into the gas one centimeter for cooling purposes. As a result, the inter-electrode spacing in the present configuration is 5 centimeters. For the data presented, 16 rows of pins with 66 pins per odd numbered row and 64 pins per even numbered row were excited. There are 21 rows of pins available on each pin board. Since the 5 downstream rows are out of the optical path, they were not excited. Each pin is ballasted with a 20000 ohm resistor and each row is ballasted with from 0 to 7500 ohms resistance. The row ballast resistors can be adjusted to vary the discharge properties in the flow direction. A schematic of the ballasting arrangement is shown in Figure 3. For the data reported here the row ballast

distribution was held constant. The distribution of resistance is shown in Figure 4. Also shown is the direction of gas flow and the extent of the optical region in the discharge.

The anode section consists of a fiberglass-epoxy plate identical in size to the cathode frame. It has embedded in it an oil cooled polished copper anode. This copper anode is 56 centimeters long in the flow direction by 135 centimeters in the optic direction and is centered on the active discharge section. The anode extends approximately 20 centimeters downstream of the last active row of pins.

MEASUREMENTS AND DATA REDUCTION

All of the data pertinent to characterizing the state of operation of the laser are recorded and processed by the NASA-Lewis central data recording computer facility. The data reported here was taken over a two day period and represents a distillation of 75 individual runs. The 75 runs were accomplished on nine different gas fills, each fill being nominally 1:7:20 (CO_2, N_2, He) at 140 torr. The loop was evacuated to 0.053N/m^2 (0.4 microns) pressure and refilled after each occurance of an arc in the discharge. During this set of runs, the velocities were varied from 73 meters per second to 130 meters per second and the average input power densities ranged from 5.66 watts/cm^3 to 15.5 watts/cm^3. Of the 136 measurements taken during each run, the 16 row currents, 16 row bus voltages, and the anode voltage are of primary interest in this report. From these recorded values one can obtain the row by row distribution of current density and discharge voltage according to the following equations,

$$V_{dis} = V_a - V_{bus} - I_{row} R_{pin} / N_{pin} \qquad (1)$$

$$j = I_{row} / A_{row} \qquad (2)$$

Equation 1 states that the discharge voltage is obtained by subtracting both the row bus voltage and the voltage drop across the pin ballast resistors from the anode voltage. The current density is obtained by dividing the row current by the discharge area seen by each row. An assumption has been made that each pin emits uniformly into a one cm^2 portion of the discharge. This assumption is not strictly valid. However, it is worth noting that the discharge footprint on the anode is not significantly larger than the outer boundaries of the active pins. Because of this

assumption, however, the current densities reported are upper bounds on the true values. From the values of j and Vdis for each row, one can easily calculate the electric field, E, the E/N ratio, the input power density, P, and the electron number density, N_e, for each row using the following equations,

$$E = (V_{dis} - 500)/G \tag{3}$$

$$E/N = (E/4.97 \times 10^{18})(T/T_o) \tag{4}$$

$$P = jE \tag{5}$$

$$Ne = j/V_d e \tag{6}$$

In Equation 3, the cathode fall voltage is taken to be 500 volts (Ref. 2). The E/N ratio calculated using Equation 4 accounts for the temperature rise of the gas as it flows through the discharge. To calculate this rise, all the power deposited into the rows upstream of the row in question was assumed to go immediately into translational energy. The downstream temperatures calculated in this manner agree with the measured downstream temperatures within five degrees centigrade. The constant in Equation 4 is the number density of the gas in the plenum tank. The electron drift velocity, V_d, used in Equation 6 was obtained from a calculation of the electron energy distribution for each particular combination of E/N and gas composition. For these calculations we have used an Air Force Weapons Laboratory computer code (Ref. 4). The calculated values of drift velocity cannot be distinguished from those presented by Lowke, et al (Ref. 5). For the range of E/N encountered during this set of tests (1.31×10^{-16} to 2.72×10^{-16} volts-cm^2) the calculated drift velocities ranged from 3.38×10^4 to 5.82×10^4 meters/second. Since the calculated current density is an upper bound, the calculated values of both power density and electron number density are also upper bounds.

RESULTS

In the following figures, the E/N ratio, current density, power density, and electron density are plotted as a function of row number (downstream position) with total discharge current and gas velocity as parameters. All of the data were obtained with the same distribution of row

ballast resistance. This particular distribution (Fig. 4) was chosen because it gave a reasonably good laser beam profile at a total discharge current of 11 amperes and a velocity of 90 m/sec.

E/N and Electric Field

Figures 5 and 6 show that the E/N ratio generally decreases as one moves downstream in the discharge. This is due to plasma from upstream rows being swept into the downstream region causing a reduction in the electric field which is required to maintain a balance between electron production and loss in the discharge. Figure 5 indicates that the electric field increases with velocity. This is most probably because convection increases the electron loss rate, and therefore a larger E/N is needed to balance generation and loss. As the current increases (Figure 6), the electric field tends to decrease except in the first two rows. This is a "preionization" phenomena; that is, conductive plasma is flowing into the region of the downstream rows and acting as an external source of electrons. At a constant velocity, a greater E/N is required to drive more current through the first two rows. The succeeding rows are "preionized" by plasma being blown downstream. With greater electron production in the first two rows, more electrons are carried down into following rows causing a reduction in the E/N at which the discharge operates. Only the first two rows appear to be operating as completely "self-sustained" discharges.

Current Density

Figures 7 and 8 illustrate the variation of current density with row number as a function of gas velocity and total current. There is very little change in the current density with velocity except that a somewhat greater current is carried in the downstream rows than the upstream rows at the higher gas velocity. The current density distribution changes dramatically as a function of total current (Figure 8). It should be remembered that the row ballast resistor values were unchanged during this series of tests. At low total current, the bulk of the current is carried in the downstream rows. The upstream rows show considerable internal (plasma) impedance and appear to be well stabilized by the gas velocity. With the low values of ballast in the upstream rows, the current rises much more rapidly than the average current but still appears to be stabilized by the gas flow. The downstream rows require resistive ballasting in addition to gas flow stabilization at all levels of

current. Subsequent tests have shown that the current could be redistributed by changing the values of the ballast resistors. The discharge seems to particularly sensitive to the values of the rows 3, 4, and 5 ballast resistors.

Power Density

Figures 9 and 10 illustrate the variation with velocity and total current of input power density in the discharge. As one would expect, the power density follows the variation in current density very closely since the spatial distribution of the electric field is nearly independent of the total current and the velocity. Since the power density is proportional to the current density (Equation 5), the data shown in the figures are upper bounds due to the assumption used in Equation 2. The maximum power density observed during this set of tests was 30 watts/cm^3.

Electron Density

The distribution of electron number density in the discharge is shown in Figures 11 and 12. One can see that as the velocity increases the electron density decreases, particularly in the first four rows. One explanation for this result is that the dependence of electron production on velocity (through E/N) is not as sensitive as the dependence of electron loss on velocity. Therefore, with increasing velocity resulting in an increased E/N for the entire discharge, the electron density would decrease. As a function of current, the electron density increases most rapidly in the first several rows. This is due to the increase in E/N which occurs in these early rows.

CONCLUSIONS

The data presented here were from the first set of measurements made on the pin-to-plate discharge in the NASA-Lewis high power laser. Even though these measurements were made at relatively low average discharge power loadings (typically 132KJ/Kg) several conclusions can be drawn which should influence the continuing evaluation of this device. First, from the dependence of current distribution on total current, it appears that the electron production in the first two rows significantly affects the current flowing in succeeding rows; a "preionization" phenomena. This combined with the velocity and spatial dependence of E/N might enable tuning the discharge to the laser kinetics. Second, it

appears that each level of total current requires its own distribution of row ballast resistor values for optimum operation. With the particular distribution of row resistors used here, the current in the first and second row are stabilized only by the gas velocity. The third and fourth rows are stabilized by the gas velocity but carry more current due to the conductive plasma which is transported into the region by the flow. As more electrons are generated in the first two rows, the current carried by rows 3 and 4 increases due to the increased plasma conductivity. The current in the last rows appears to be limited by the ballast resistors at all levels of current.

Additional work needed to characterize pin-to-plate flowing gas discharges include the following:

1. A direct measurement of the electron density would check the validity of the assumptions used in the calculations.

2. The effect of the power input distribution on the laser output beam profile should be examined to determine the optimum row ballast resistor values for each level of current.

3. The effect of adding or deleting rows of pins upstream or downstream of the present discharge should be examined to determine the optimum method of putting power into the optical region of the laser.

SYMBOLS

A_{row}	discharge area seen by one row, cm^2
e	electron charge, 1.591×10^{-19} A-sec.
E	electric field, volts/cm
E/N	ratio of electric field to neutral gas density, volts-cm^2
G	discharge gap, cm
I_{row}	row current, A
j	discharge current density, A/cm^2
N_e	electron number density, cm^{-3}
N_{pin}	number of pins per row
P	discharge input power density, $watts/cm^3$
R_{pin}	pin ballast resistor value, 20000ohms
T	local static temperature, ^oK
T_o	plenum static temperature, ^oK
V_a	anode voltage, volts
V_{bus}	row voltage, volts
V_d	electron drift velocity, cm/sec

V_{dis} discharge voltage, volts

REFERENCES

1. W. J. Weigan, M. C. Fowler, and J. A. Benda, Appl. Phys. Lett., vol. 18, 365 (1971).

2. S. A. Wutzke, and J. L. Pack, J. L., Post deadline paper, IEEE/OSA 4th. Conference on Laser Engineering and Applications, Washington, D.C., May 1973.

3. R. E. Lancashire, D. L. Alger, E. J. Manista, J. G. Slaby, J. W. Dunning, Jr., and R. M. Stubbs, The NASA High-Power Carbon Dioxide Laser -. Versitile Tool for Laser Applications. NASA TM X-73485, 1976.

4. T. J. Ernst, private communication (see also J. C. Rich, and R. K. Parsons, eds, Laser Digest - Fall, 1973, AFWL-TR-73-23, Dec. 1973.)

5. J. J. Lawke, A. V. Phelps, and B. W. Irwin, J. Appl. Phys., 44, 4664 (1973).

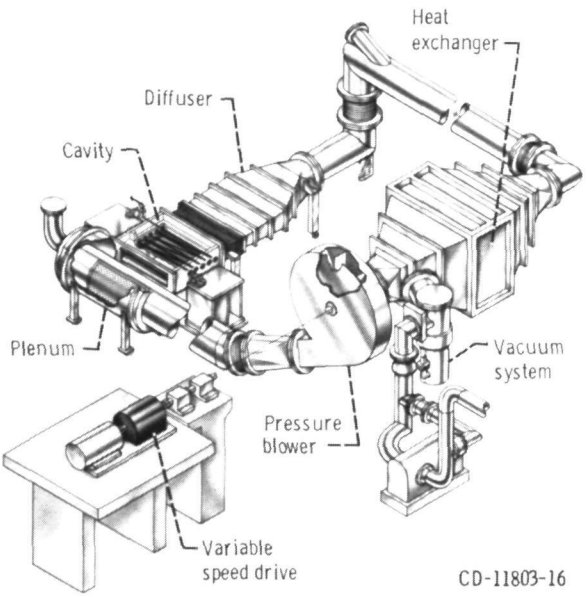

Figure 1. - Drawing of the NASA-Lewis high-power laser.

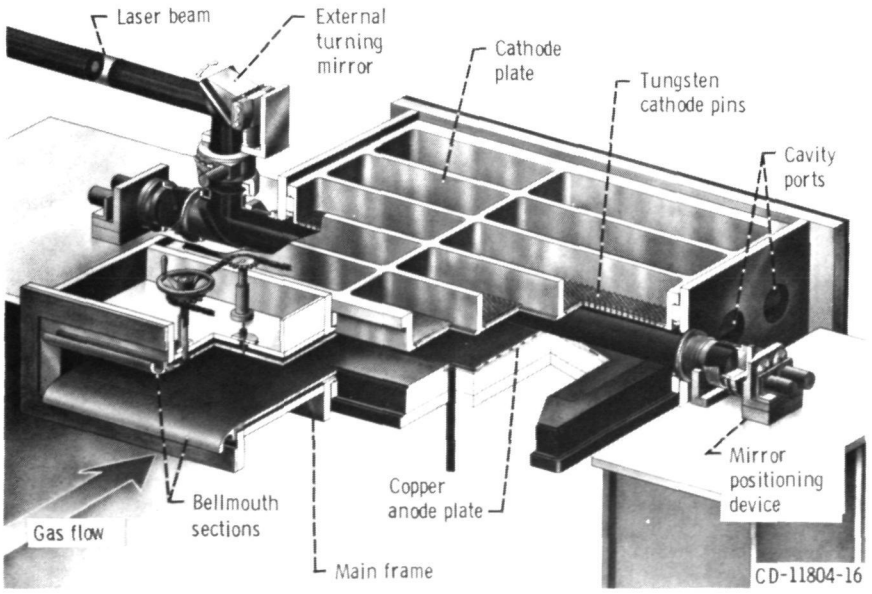

Figure 2. - Drawing of the laser test cavity with pin-to-plane self-sustained discharge.

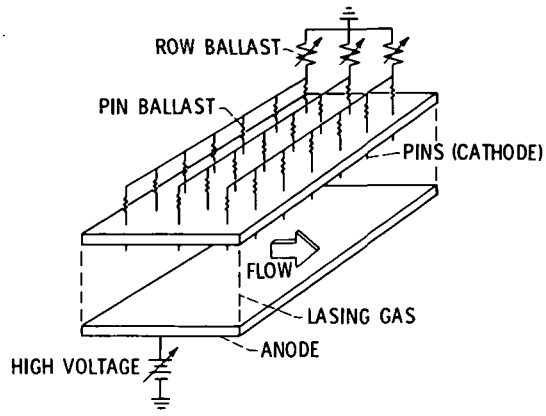

Figure 3. - Schematic of electrodes and discharge for pin-to-plane discharge.

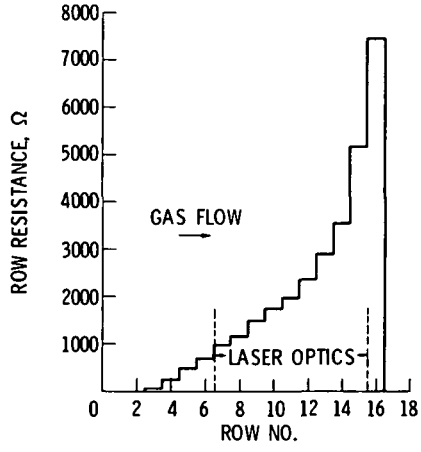

Figure 4. - Distribution of row resistor values.

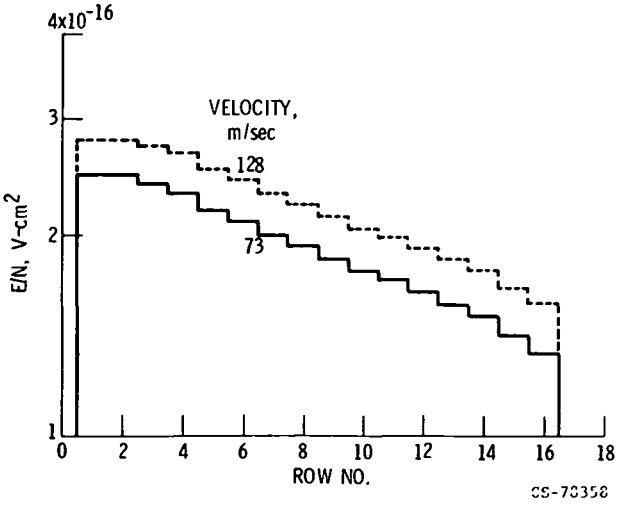

Figure 5. - Distribution of E/N as a function of downstream position with gas velocity as a parameter.

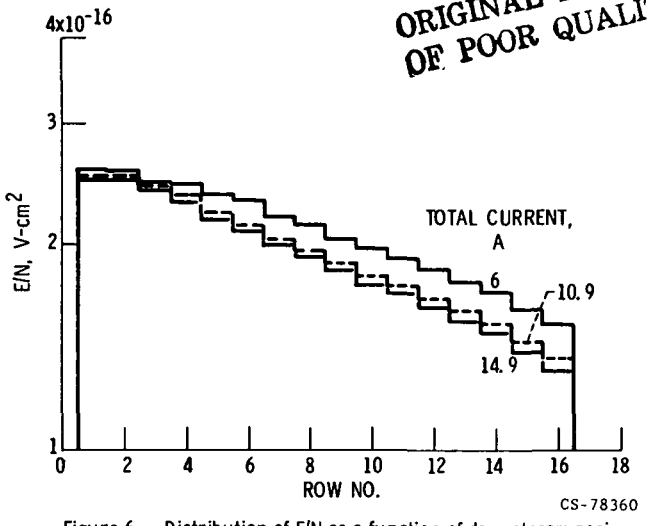

Figure 6. - Distribution of E/N as a function of downstream position with total discharge current as a parameter.

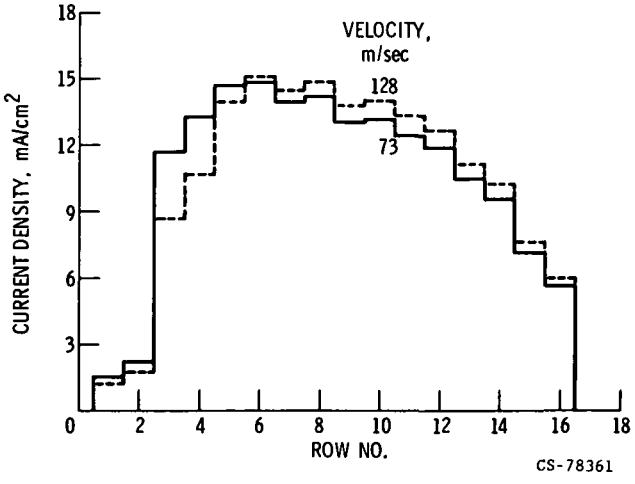

Figure 7. - Distribution of current density as a function of downstream position with gas velocity as a parameter.

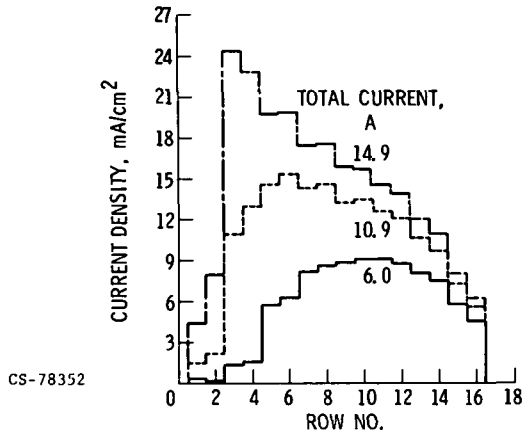

Figure 8. - Distribution of current density as a function of downstream position with total discharge current as a parameter.

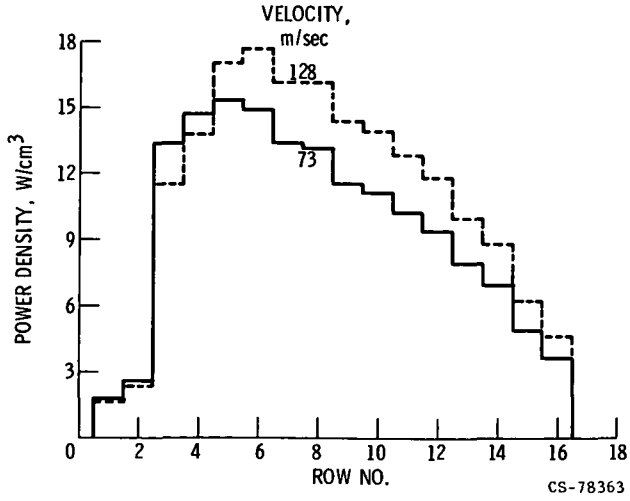

Figure 9. - Distribution of input power density as a function of downstream position with gas velocity as a paremeter.

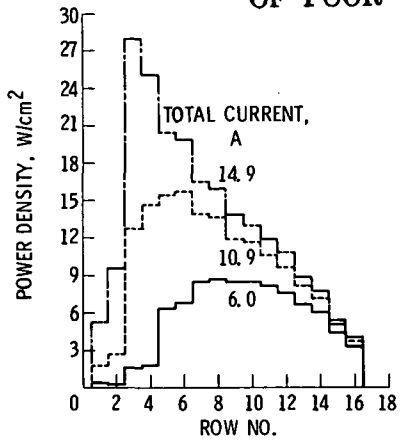

Figure 10. - Distribution of input power density as a function of downstream position with total discharge current as a parameter.

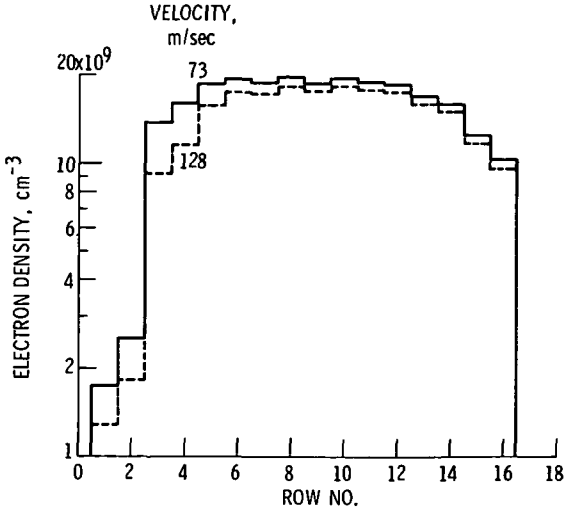

Figure 11. - Distribution of electron density as a function of downstream position with gas velocity as a parameter.

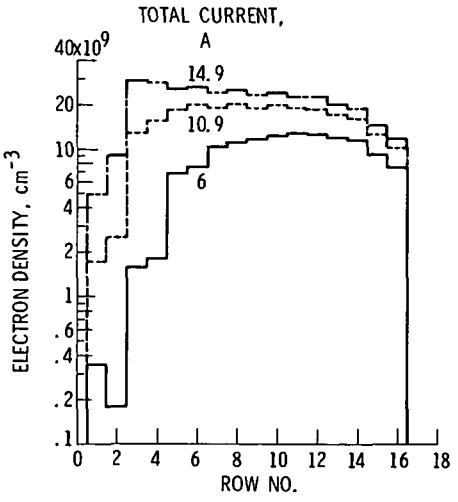

Figure 12. - Distribution of electron density as a function of downstream position with total discharge current as a parameter.

NATIONAL AERONAUTICS AND SPACE ADMINISTRATION
WASHINGTON, D.C. 20546

OFFICIAL BUSINESS
PENALTY FOR PRIVATE USE $300

SPECIAL FOURTH-CLASS RATE BOOK

POSTAGE AND FEES PAID
NATIONAL AERONAUTICS AND SPACE ADMINISTRATION
451

POSTMASTER: If Undeliverable (Section 158 Postal Manual) Do Not Return